31st Annual International Conference of the IEEE EMBS
Minneapolis, Minnesota, USA, September 2-6, 2009

Shape-Aided Kidney Extraction in MR Urography

Yang Tang, *Member, IEEE*, Hollie Jackson, Susan Lee, Marvin Nelson, Rex A. Moats

***Abstract*—MR Urography (MRU) plays an important role in pediatric renal diagnoses. While accurate measurement of the kidney is essential for each imaging study, it is challenging to extract the kidney from its background. In this paper, we propose a co-focus elliptical kidney model (CEKM) to integrate the shape prior and build a novel extraction method with both regional and edge information. With a similarity metric defined between a binary mask and CEKM, a kidney template can be obtained using optimization technique. Then, a shape term derived from a distance and orientation description is designed to modify an active contour model. The distance map is used to control the contours in terms of CEKM and orientation map is designed to reduce the artifacts resulting from fake edges. The final kidney was determined with iterative solution. With the priori shape description in a parametric space, the new method can precisely extract the kidney without training, and supply promising results as the experiments demonstrated.**

I. Introduction

KINDEY disorders are common in pediatric urology and many clinical decisions are partially made based on imaging results. In the long term, MR Urography (MRU) has the potential to become a routine diagnostic tool because it lacks the radiation exposure complications of nuclear medicine and CT modalities.

Using dynamic contrast enhanced magnetic resonance imaging (DCE-MRI), MRU can provide both the functional and anatomic information for pediatric diagnoses. In the quantitative analysis, kidney size is highly correlated with the renal functional reserve. Nearly all diagnosis for renal disease undergoes an imaging examination that assesses the kidney health by extracting the kidney region.

Excluding surrounding background from kidney is a challenging task. Due to the very short TR and TE setting in practical sequence, high signal to noise rate (SNR) is hard to achieve. Also, contrast agent leakage from artery to nearby organs often occurs, which complicates the objective region extraction. Due to the limited resolution, partial volume problem often blurs the contour between different tissues. Furthermore, the inhomogeneity phenomenon increases the uncertainty. Also, the movement caused by respiration cannot be ignored. For the motion artifacts, the registration technique [1] can be employed before the segmentation, which is not included in this paper.

To perform the segmentation task, methods are proposed based on different criterion than have been previously described. Threshold methods are both imposed on one image at a particular time point [2] or the post-pre image (post-contrast image subtract pre-contrast image) [3]. Only threshold based methods have limited capacity to deal with noises, and segment also was performed to include the entire kidney morphology. For example, H-maxima morphological transform explored to sever connection with surrounding tissues and extract the cortex in MRU [4]. Based on the surrounding rectangle and edge information, H-maxima method offers the radiologist a good semi-automatic method to delineate the kidney.

Differing from static imaging, MRU supply the dynamic information for each pixel. Instead of post-pre image, the whole time intensity curve (TIC) also served as criterion within varying frameworks. Chevaillier [5] used a K mean method to classify the TICs. Similar work also can rely on a neural network [6]. Song [7] put the 4D data to a level set framework, which deals with the spatial and temporal dimensions at the same time. Graphic cut also supplies an effective way of clustering kidney related pixels and the performance has been evaluated for MR Renography [8].

However, in practice, we found only intensity and spatial information sometime does not produce satisfactory segmentation in clinic MRU data. In this study, we incorporate the shape knowledge into the segment framework and propose a shape model to aid the kidney extraction.

II. Method

A. Overview

Our method is performed in two stages. The purpose of first stage is a rough extraction of kidney area by matching a co-focus elliptical model to a binary mask using optimization in the parametric space. Because the similarity metric is defined on their overlap of regions, we call it as a region stage. In the second stage, extraction is refined. With an initial contour generated from the previous kidney template, Contour is iteratively approached by deforming an active contour model. A shape term is designed to punish the deviation from the shape prior in this step. The contour is deformed mainly based on the edge information in the image and it is called an edge stage.

The general work flow is summarized in Fig.1.

Manuscript received April 7, 2009.

Yang Tang, Hollie Jackson, Marvin Nelson Jr, Rex Moats are with the Department of Radiology, University of Southern California and Keck School of Medicine, Los Angeles, California 90027, USA. (e-mail: ytang, hjachson, mdnelson, rmoats@ chla.usc.edu).

Susan.Lee is with the Department of biomedical engineering, University of Southern California and Keck School of Medicine, Los Angeles, California 90027, USA.(e-mail:slee@chla.usc.edu)

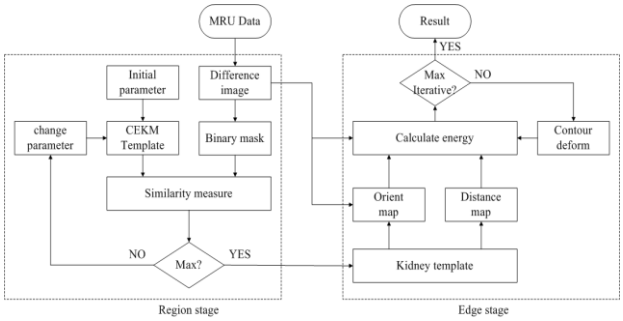

Fig.1.method workflow

B. Co-focus elliptical kidney model (CEKM)

To simulate the organ or object's shape, the ellipse and its derivatives are widely used in medical image analysis [9][10]. Motivated by previous work, a co-focus elliptical kidney model (CEKM) is proposed here to describe the renal shape.

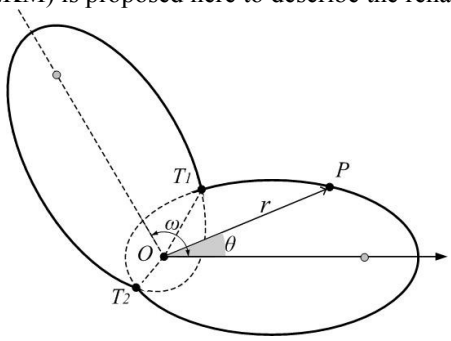

Fig.2.co-focus ellipse model

Co-focus ellipse is defined as two ellipses with one shared focus. As Fig.2 shows, we set one ellipse horizontally; another deviated ellipse rotated around one focus in a counter-clockwise direction. The deviation angle, ω, is the angle between the two major axes. We use the ellipse polar equation with one focus at the origin. The horizontal ellipse and rotated ellipses are:

$$r_1(\theta) = \frac{a_1(1-\varepsilon_1^2)}{1+\varepsilon_1\cos\theta},$$

$$r_2(\theta) = \frac{a_2(1-\varepsilon_2^2)}{1+\varepsilon_2\cos(\theta+\omega)} \quad (1)$$

Co-focus ellipse can be written as the combination of two ellipses as:

$$r(\theta) = r_1(\theta), \quad \theta \in [0,\tau_1] \cup [\tau_2.2\pi]$$
$$r(\theta) = r_2(\theta), \quad \theta \in [\tau_1,\tau_2] \quad (2)$$

Where τ_1 and τ_2 are angles corresponding to the diverging point and converging points (marked as T_1 and T_2 respectively in Fig.2.). Considering the positional information (only rotation and translation included in this study), the CEMK in Cartesian coordinates can be defined as:

$$CEMK = \begin{bmatrix} c_x \\ c_y \end{bmatrix} + rot(\varphi)P \quad (3)$$

Here c_x, c_y denote a translation, $rot(\varphi)$ is a rotation matrix and P is the point on the co-focus ellipses. From (1)(2)(3), a CEKM is defined adequately with 8 parameters and vectors in parametric space are sufficient to control the deformation.

CEKM has advantages to simulate kidney in general firstly because it has an analytical expression and can control the fitting in a parametric space without training. Also, the two ellipses in CEMK can easily describe the different curvature in dual poles, and the concave region in the joint regions. With the deviation angle in different directions, the right and left kidney can be easy simulated. And the ellipse or circle templates can be considered as special cases of CEKM by decay their parameters.

C. Region stage

In the regional stage, to match a CEKM to the kidney image, we need to define a similarity metrics and assign it to the framework of optimization.

A similarity metric is typically defined as the distance between reference and target objects. These distances are often defined by the gradients of their edges or histogram features of these regions. However, these metrics seems to be unsuitable for kidney segmentation. Because the kidney is composed of multiple tissues, each of them reveals edges in a different time frame, which leads to abundant edges near the kidney contour. It is particularly obvious in a lesion kidney with a thin cortex. For the histogram metrics, the statistical intensity knowledge of the region varies significantly between normal and lesion kidneys, even in different slices of the same kidney. Therefore, we used a binary mask with the metric defined as mean overlap (*MO*) of object areas.

$$MO = \frac{2*\left|Mask_{CEKM} \cap Mask_{\mathrm{Image}}\right|}{\left|Mask_{CEKM}\right| + \left|Mask_{\mathrm{Image}}\right|} \quad (4)$$

For the binary mask of kidney image, a p-threshold method is utilized to take the prior size knowledge into account. Because the mean overlap between binary masks supplies a relatively robust criterion for matching, a simplex solution based on gradient descent is utilized to find the maximum in parametric space. Also, global optimization method (e.g. simulated annealing [11]) is useful to prevent falling into local minima. Other prior knowledge of kidney for most humans can also be incorporated. For example, the kidneys are nearly in the same position and similar size. The initial parameter can be decided empirically by adding the constrained boundary for parameters.

D. Edge stage

In this stage, further refinement is performed with an active contour model [12] on the post-pre image based on the edge information. To use the kidney template resulting from the first stage, a shape term is designed, which includes a distance map and an orientation map. The first part is to keep the edges near the template and second one is to reduce the distortion caused by nearby fake edges.

A distance map describes serial iso-contours of difference distance from the template contour. To allow the individual variance of kidney surface, we set a reliant range near

template. When inside this range, the weight decays relatively slowly. However, the weight reduces quickly outside the reasonable field. With a logistic function, the distance probabilistic function can be defined as:

$$w_{dst} = \frac{1}{1 - e^{(|d|-b)}/\mu} \tag{5}$$

Where b controls the reasonable range and μ adjusts the slope of range's boundaries.

In some of the diseased kidneys, there are dysfunctional areas inside kidney, which results in undesired inner contours. Because these fake edges have small distances to the real contour, they are difficult to be distinguished only by distance map. However, according to Fig.3, we find the real and fake edges can be discriminated by the coincidence of their directions with the template.

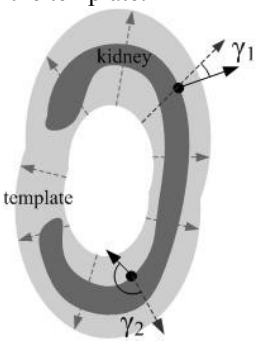

Fig.3. orientation map

A cosine function is utilized to measure their orientation divergence, which preserves same directions to 1 and punish inverse directions to 0.

$$w_{ort} = (1 + \cos\gamma)/2 \tag{6}$$

Thus, the shape term can be defined by combining the (5) and (6) as:

$$W(x(s)) = w_{dst}(x(s)) \cdot w_{ort}(x(s)) \tag{7}$$

Equation (7) acts as a penalty term in the traditional active contour model as following shows:

$$E = \int_{curve} (E_{\text{int}}(x(s)) + W(x(s)) \cdot E_{ext}(x(s)))\, ds \tag{8}$$

Here, E_{int} and E_{ext} represent the internal and external image energy, respectively. Equation (8) can be solved by an iterative schedule.

III. Experiments and Results

The method was implemented on a PC and tested on slices from 6 clinical MRU datasets. In the following experiments, the raw data in early enhanced phases were selected as a reference background. Initial curves are marked by white color, matched templates are in red color and final contours are blue.

A. Image Acquisition

For kidney diagnosis, coils are put near the abdomen area. A dynamic MRI with 3D coronal fast GRE sequence was performed on a 1.5 Tesla system. The flip angle is 45°, and TR ranged from 6 to 6.7ms, TE ranged 0.83 to 1.22ms.

B. Initial position

We discuss the sensitivity of the matched template in terms of the start point--a contour generated by an initial vector in parametric space.

Experiments are carried out in different kidneys with several start points. Representative parts of the experiments are shown in Fig.4.

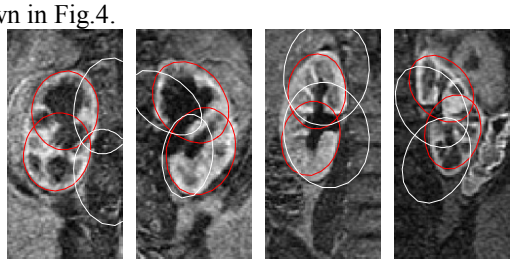

Fig.4. different start points

It was found that with the binary regional similarity metric, the template was not very sensitive to the start points and has a relatively large capturable range in most of the cases. Therefore, the local optimization methods can satisfy most requirements. We also observed that when the start points are far from the target or a poor binary mask is produced, the local optimization will fail. In such cases, the global methods are preferred.

C. Shape term

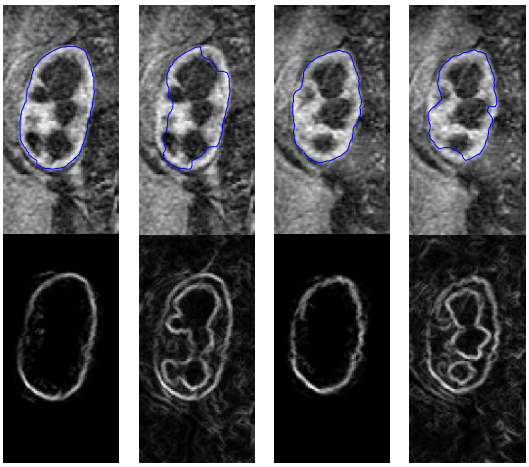

(a) (b) (c) (d)

Fig.5. effects of orientation map

Fig. 5 is from a ten month old patient with Ureterpelvic junction obstruction (UPJ). Due to the short infundibula and dilatation of renal pelvis, some tissues inside the kidney are dysfunctional, which remained un-enhanced throughout the dynamic imaging. The first row of Fig.5 presented two nearby slices, and the thin cortex can be found surrounding the kidney surface. With the same initial matched template, the curve was refined by the active contour model. Fig. 5a and c exhibits the results with the shape term. Without the shape term, the curves tend to cling to some undesirable edges (Fig.5b and d). The second row showed the corresponding external energy in (8). The distance and

orientation map in the shape term can effectively increase order and help deform the shape to the right position.

D. Compare with manual results

To evaluate the results, we compared our method with the manual operation. Overlap percent (OP) was used for similarity measurement between region of manual(R_M) and automatic(R_A).

$$OP = \frac{1}{2}\left(\frac{|R_M \cap R_A|}{|R_M|} + \frac{|R_M \cap R_A|}{|R_A|}\right)$$

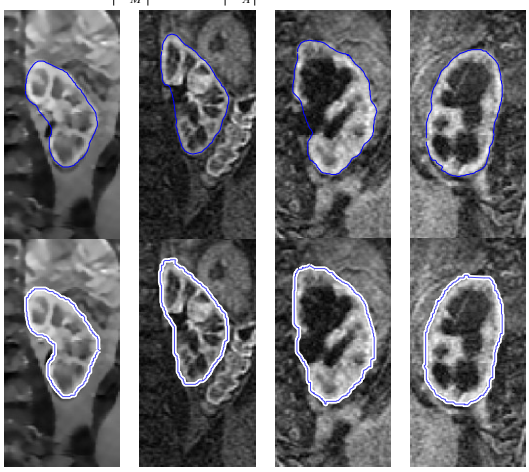

(a) (b) (c) (d)

Fig.6 compare with manual results

The statistical evaluation showed the OP is more than 95%. Part results of both healthy and diseased kidneys are shown in Fig.6. The first row is from shape aided method, and corresponding manual results are in second row. We observe that the contour described by the computations near the cortex is more precise than manual results. The main extra overlap area lies in the pelvis or lesion region, especially in some dilated unhealthy kidneys.

E. 3D reconstruction

We also tried the method in a full 3D clinic dataset. The typical slice (near the middle of kidney) can be chosen empirically by slice index [4]. For 3D segmentation, a slice-by-slice strategy is performed. However, in 3D case, the CEMK is unnecessary to be constructed and deformed for each slice. The extracted contour of nearby slice can act as the initial position for next slice. The reconstructed result is show as Fig.7.

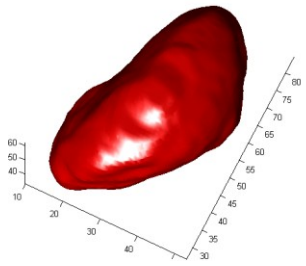

Fig7. 3d reconstruction

IV. Conclusion

A kidney extraction method with shape prior is described in this paper. As demonstrated by the experiments, this shape-aided kidney extraction method provided promising results in the clinical MRU data with low image quality. Nonetheless, limitations still exist. It is limited for the coronal images. Also it does not work for some severely diseased kidneys, where most of the cortex is dysfunctional. We try to figure out their boundary according to the compartment information of neighbor tissues in future.

References

[1] Sun, Y., Jolly, M.P., Mourua, J.M., "Integrated registration of dynamic renal perfusion MR images". In Proc. IEEE ICIP, pp. 1923–1926. IEEE Computer Society Press, Los Alamitos 2004.

[2] J. D. G. Smith, et.al, "MR imaging of kidneys: functional evaluation using F-15 perfusion imaging", Pediatr Radiol, pp293–304,2003.

[3] J.A. Priester, A.G. Kessels, et.al, "MR renography by semiautomated image analysis: performance in renal transplant recipients", J Magn Reson Imaging. pp134–140, 2001.

[4] Koh,H.K. Weijia Shen, Shuter, B. Kassim,A.A., segmentation of kidney cortex in MRI studies using a constrained morphological 3D H-maxima Transform, Control, Automation, Robotics and Vision, 9th International Conference, Singapore.

[5] B. Chevaillier, Y. Ponvianne, et.al, "Functional semiautomated segmentation of renal dce-mri sequences", IEEE International Conference on Acoustics, Speech and Signal Processing, Las Vegas, 2008.

[6] B. Chevaillier, Y. Ponvianne, et.al, "Functional semi-automated segmentation of renal DCE-MRI sequences using a Growing Neural Gas algorithm", 16th European Signal Processing Conference,Lausanne, 2008.

[7] T. Song, V. S. Lee, et.al, "Segmentation Of 4D MR Renography Images Using Temporal Dynamics In A Level Set Framework", 5th IEEE International Symposium on Biomedical Imaging: From Nano to Macro, 2008.

[8] Henry Rusinek,et.al, "Performance of an automated segmentation algorithm for 3D MR renography", Magnetic Resonance in Medicine Volume 57 Issue 6, Pages 1159 - 1167.

[9] Pang B, Zhang D, Wang K. "The bi-elliptical deformable contour and its application to automated tongue segmentation in Chinese medicine". IEEE Trans Med Imaging 2005;24(8):946-56.

[10] Pu J, Zheng B, Leader JK, Gur D. "An ellipse-fitting based method for efficient registration of breast masses on two mammographic views". Med Phys. 2008 Feb;35(2):487-94.

[11] G. Storvik, "A Bayesian approach to dynamic contours through stochastic sampling and simulated annealing", IEEE Trans. Pattern Anal. Machine Intell., vol. 16, no. 10, pp. 976–986, Oct. 1994.

[12] M. Kass, A. Witkin, and D. Terzopoulos, "Snakes: Active contour models", in Proc. Int. Conf. Computer Vision, 1987, pp. 259–269.